JOC Article

Transition States for the Dimerization of 1,3-Cyclohexadiene: A DFT, CASPT2, and CBS-QB3 Quantum Mechanical Investigation†

Daniel H. Ess,‡ Amy E. Hayden,‡ Frank-Gerrit Klärner,§ and K. N. Houk*,‡

Department of Chemistry and Biochemistry, University of California, Los Angeles, California 90095, and Institut für Organische Chemie der Universität Duisburg-Essen, 45117 Essen, Germany

houk@chem.ucla.edu

Received May 31, 2008

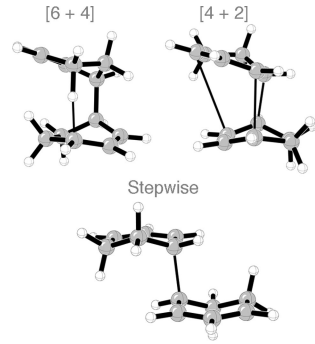

Quantum mechanical calculations using restricted and unrestricted B3LYP density functional theory, CASPT2, and CBS-QB3 methods for the dimerization of 1,3-cyclohexadiene (**1**) reveal several highly competitive concerted and stepwise reaction pathways leading to [4 + 2] and [2 + 2] cycloadducts, as well as a novel [6 + 4] ene product. The transition state for *endo*-[4 + 2] cycloaddition (***endo*-2TS**, $\Delta H^{\ddagger}_{\text{B3LYP(0K)}} = 28.7$ kcal/mol and $\Delta H^{\ddagger}_{\text{CBS-QB3(0K)}} = 19.0$ kcal/mol) is not bis-pericyclic, leading to nondegenerate primary and secondary orbital interactions. However, the C_s symmetric second-order saddle point on the B3LYP energy surface is only 0.3 kcal/mol above ***endo*-2TS**. The activation enthalpy for the concerted *exo*-[4 + 2] cycloaddition (***exo*-2TS**, $\Delta H^{\ddagger}_{\text{B3LYP(0K)}} = 30.1$ kcal/mol and $\Delta H^{\ddagger}_{\text{CBS-QB3(0K)}} = 21.1$ kcal/mol) is 1.4 kcal/mol higher than that of the *endo* transition state. Stepwise pathways involving diallyl radicals are formed via two different C−C forming transition states (***rac*-5TS** and ***meso*-5TS**) and are predicted to be competitive with the concerted cycloaddition. Transition states were located for cyclization from intermediate ***rac*-5** leading to the *endo*-[4 + 2] (***endo*-2**) and *exo*-[2 + 2] (***anti*-3**) cycloadducts. Only the *endo*-[2 + 2] (***syn*-3**) transition state was located for cyclization of intermediate ***meso*-5**. The novel [6 + 4] "concerted" ene transition state (***threo*-4TS**, $\Delta H^{\ddagger}_{\text{UB3LYP(0K)}} = 28.3$ kcal/mol) is found to be unstable with respect to an unrestricted calculation. This diradicaloid transition state closely resembles the cyclohexadiallyl radical rather than the linked cyclohexadienyl radical. Several [3,3] sigmatropic rearrangement transition states were also located and have activation enthalpies between 27 and 31 kcal/mol.

Introduction

The cycloaddition reaction continues to be a powerful and versatile carbon−carbon bond-forming reaction to construct natural products[1] and materials.[2] Also, cycloaddition reactions continue to provide a source of data with which reactivity and selectivity principles can be developed.[3] Several recent conceptual breakthroughs in cycloaddition chemistry have stimulated great interest in Diels−Alder dimerization reactions.[4] Caramella and co-workers discovered that *endo*-cyclopentadiene dimerization occurs via a single, highly asynchronous, "bis-pericyclic" Diels−Alder transition state.[4a] After this bis-pericyclic transition state, the shared reaction pathway splits (bifurcates), leading to either the [4 + 2] or [2 + 4] cycloadduct. Another important conceptual breakthrough for pericyclic processes is the idea of "para-intermediates," intermedi-

† Dedicated to Professor William von Eggers Doering on the occasion of his 91st birthday.
‡ University of California, Los Angeles.
§ Institut für Organische Chemie der Universität Duisburg-Essen.

10.1021/jo8011804 CCC: $40.75
Published on Web 09/03/2008

ates with short lifetimes that do not differ greatly in energy from the transition state, resulting in a plateau-like potential energy surface.[5]

Although the dimerization of cyclopentadiene, 1,3-butadiene, and heterodiene analogs have been extensively investigated,[6] the thermal dimerization of 1,3-cyclohexadiene, **1**, has not been explored computationally.[7] The dimerization of **1** gives primarily the *endo*-[4 + 2] cycloadduct (***endo*-2**). However, significant amounts of *exo*-[4 + 2] and [2 + 2] cycloadducts as well as a novel [6 + 4] ene reaction product were also observed (Scheme 1, see Results and Discussion).[8] Several intriguing questions about the mechanism of this reaction warranted our computational exploration: (1) Does *endo* cycloaddition proceed through a bis-pericyclic transition state? (2) What is the nature of the intermediates involved in the stepwise processes and how are they related on the potential energy surface? (3) Does the [6 + 4] ene reaction product result from a concerted or stepwise pathway? Here we report our investigation of cyclohexadiene dimerization using the correlated composite ab initio CBS-QB3, the multireference CASPT2, and B3LYP density functional theory (DFT) methods.

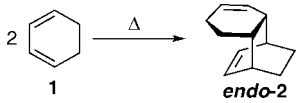

Computational Methods

All stationary points (gas phase optimized) were verified as minima or first-order saddle points by calculation of the full Hessian at (U)B3LYP/6-31G(d) or RB3LYP/6-311G(d,p) (CBS-QB3 geometries) using Gaussian03.[9] All energies presented are B3LYP $\Delta H_{(0K)}$ values relative to separated reactants and include zero-point energy (unscaled). All $\Delta H_{(298)}$ values include translational, rotational, and vibrational and pV correction terms. $\Delta G_{(298)}$ values include a $-298\Delta S$ term. For diradical species, spin-projected values (E^{SP}) were calculated using the Yamaguchi and Houk procedure outlined in eqs 1 and 2 below.[10] Reported B3LYP enthalpies using spin-projected energies include zero-point energy correction.

$$E^{SP}_{singlet} = E_{singlet} + [\chi(E_{singlet} - E_{triplet})] \quad (1)$$

$$\chi = \frac{\left({}^1\langle S^2\rangle / {}^3\langle S^2\rangle\right)}{1 - \left({}^1\langle S^2\rangle / {}^3\langle S^2\rangle\right)} \quad (2)$$

All CASPT2(8,8) energy evaluations were performed on UB3LYP/6-31G(d) structures. This second-order perturbation CASPT2 method provides a balance of dynamical and nondynamical (multireference) electron correlation.[11] All CASPT2 calculations were carried out using MOLCAS version 6.2 with an (8,8) active space and 6-31G(d) basis set. The active space incorporated the four doubly degenerate π-orbitals of cyclohexadiene and the corresponding orbitals of the transition states and diradical intermediates.

The CBS-QB3[12] composite method uses an extrapolation procedure of MP2 pairwise correlation effects designed to remove basis set truncation error. On a B3LYP/6-311G(d,p) geometry, the following energy corrections are used to give a final CBS-QB3 energy ($E^{CBS\text{-}QB3}$):

$$\begin{aligned} E^{CBS\text{-}QB3}(H_{(0K)}) = {} & E(\text{MP2/6-311+G(2df,2p))} - \\ & \text{CBSB7)} + E(\text{MP2 CBS extrapolation}) + \\ & E(\text{MP4(SDQ)/6-31+G(d,p)} - \text{CBSB4}) - \\ & E(\text{MP2/6-31G+(d,p)} - \text{CBSB4}) + \\ & E(\text{CCSD(T)/6-31+G}^{\dagger}) - \\ & E(\text{MP4(SDQ)/6-31+G}^{\dagger}) + \\ & E_{ZPE}(\text{B3LYP/6-311G(d,p)}) + \\ & E(\text{int}) + E(\text{empirical}) \end{aligned} \quad (3)$$

For hydrocarbon pericyclic reactions, CASPT2 and CBS-QB3 have mean absolute deviations of 2.3 and 2.8 kcal/mol, respectively,

(1) (a) Yu, M.; Danishefsky, S. J. *J. Am. Chem. Soc.* **2008**, *130*, 2783–2785. (b) Balskus, E. P.; Jacobsen, E. N. *Science* **2007**, *317*, 1736–1740. (c) Singh, R. P.; Bartelson, K.; Wang, Y.; Su, H.; Lu, X.; Deng, L. *J. Am. Chem. Soc.* **2008**, *130*, 2422–2423. (d) Winbush, S. M.; Mergott, D. J.; Roush, W. R. *J. Org. Chem.* **2008**, 1818–1829. (e) Leca, D.; Gaggini, F.; Cassayre, J.; Loiseleur, O.; Pienizaek, S. N.; Luft, J. A. R.; Houk, K. N. *J. Org. Chem.* **2007**, *72*, 4284–4287. (f) Snyder, S. A.; Corey, E. J. *J. Am. Chem. Soc.* **2006**, *128*, 740–742. (g) Lu, J.-Y.; Arndt, H.-D. *J. Org. Chem.* **2007**, *72*, 4205–4212. (h) Lebold, T. P.; Kerr, M. A. *Org. Lett.* **2007**, *9*, 1883–1886.

(2) (a) McNeil, A. J.; Muller, P.; Whitten, J. E.; Swager, T. M. *J. Am. Chem. Soc.* **2006**, *128*, 12426–12427. (b) Ishow, E.; Bouffard, J.; Kim, Y.; Swager, T. M. *Macromolecules* **2006**, *39*, 7854–7858. (c) Chuang, S.-C.; Sander, M.; Jarrosson, T.; James, S.; Rozumov, E.; Khan, S. I.; Rubin, Y. *J. Org. Chem.* **2007**, *72*, 2716–2723. (d) Sander, M.; Jarrosson, T.; James, S.; Rozumov, E.; Khan, S. I.; Rubin, Y. *J. Org. Chem.* **2007**, *72*, 27124–27131. (e) Mitzi, D. B.; Afzali, A. *Cryst. Growth Des.* **2007**, *7*, 691–697. (f) Szalai, M. L.; McGrath, D. V.; Wheeler, D. R.; Zifer, T.; McElhanon, J. R. *Macromolecules* **2007**, *40*, 818–823. (g) Perepichka, D. F.; Bendikov, M.; Meng, H.; Wudl, F. *J. Am. Chem. Soc.* **2003**, *125*, 10190–10191. (h) Chen, X.; Wudl, F.; Mal, A. K.; Shen, H.; Nutt, S. R. *Macromolecules* **2003**, *36*, 1802–1807.

(3) (a) Dai, M.; Sariah, D.; Yu, M.; Danishefsky, S. J.; Jones, G. O.; Houk, K. N. *J. Am. Chem. Soc.* **2007**, *129*, 645–657. (b) Gordillo, R.; Dudding, T.; Anderson, C. D.; Houk, K. N. *Org. Lett.* **2007**, *9*, 501–503. (c) Barluenga, J.; Fernadez-Rodriguez, M. A.; Garcia-Garcia, P.; Aguilar, E. *J. Am. Chem. Soc.* **2008**, *130*, 2764–2765. (d) Takagi, R.; Miyanaga, W.; Tojo, K.; Tsuyumine, S.; Ohkata, K. *J. Org. Chem.* **2007**, *72*, 4117–4125. (e) Domingo, L. R.; Aurell, M. J.; Arno, M.; Saez, J. A. *J. Org. Chem.* **2007**, *72*, 4220–4227. (f) Acevedo, O.; Jorgensen, W. L.; Evanseck, J. D. *J. Chem. Theory Comput.* **2007**, *3*, 132–138. (g) Berski, S.; Andres, J.; Silvi, B.; Domingo, L. R. *J. Phys. Chem. A* **2006**, *110*, 13939–13947.

(4) (a) Caramella, P.; Quadrelli, P.; Toma, L. *J. Am. Chem. Soc.* **2002**, *124*, 1130–1131. (b) Celebi-Olcum, N.; Ess, D. H.; Aviyente, V.; Houk, K. N. *J. Am. Chem. Soc.* **2007**, *129*, 4528–4529.

(5) (a) Northrop, B. H.; Houk, K. N. *J. Org. Chem.* **2006**, *71*, 3–13, and references therein. (b) Leach, A. G.; Goldstein, E.; Houk, K. N. *J. Am. Chem. Soc.* **2003**, *125*, 8330–8339. (c) Zhao, Y.-L.; Suhrada, C. P.; Jung, M. E.; Houk, K. N. *J. Am. Chem. Soc.* **2006**, *128*, 11106–11113. (d) Caramella, P.; Quadrelli, P.; Toma, L.; Romano, S.; Khuong, K. S.; Northrop, B.; Houk, K. N. *J. Org. Chem.* **2005**, *70*, 2994–3008. (e) Khuong, K. S.; Jones, W. H.; Pryor, W. A.; Houk, K. N. *J. Am. Chem. Soc.* **2005**, *127*, 1265–1277.

(6) (a) Toma, L.; Romano, S.; Quadrelli, P.; Caramella, P. *Tetrahedron Lett.* **2001**, *42*, 5077–5080. (b) Quadrelli, P.; Romano, S.; Toma, L.; Caramella, P. *Tetrahedron Lett.* **2002**, *43*, 8785–8789. (c) Quadrelli, P.; Romano, S.; Toma, L.; Caramella, P. *J. Org. Chem.* **2003**, *68*, 6035–6038. (d) Lasorne, B.; Dive, G.; Desouter-Lecomte, M. *J. Chem. Phys.* **2005**, *122*, 184304. (e) Dinadayalane, T. C.; Sastry, G. N. *Organometallics* **2003**, *22*, 5526–5533. (f) Dinadayalane, T. C.; Gayatri, G.; Sastry, G. N.; Leszczynski, J. *J. Phys. Chem. A* **2005**, *109*, 9310–9323.

(7) (a) Gagnepain, J.; Castet, F.; Quideau, S. *Angew. Chem., Int. Ed.* **2007**, *46*, 1533–1535. (b) Gagnepain, J.; Méreau, R.; Dejugnac, D.; Léger, J.-M.; Castet, F.; Deffieux, D.; Pouységu, L.; Quideau, S. *Tetrahedron* **2007**, *63*, 6493–6505.

(8) (a) Klärner, F.-G.; Dogan, B. M. J.; Ermer, O.; Doering, W. v. E.; Cohen, M. P. *Angew. Chem., Int. Ed. Engl.* **1986**, *25*, 108–110. (b) de Maré, G. R.; Huybrechts, G.; Toth, M.; Goldfiner, P. *Trans. Farad. Soc.* **1971**, *67*, 1397–1400. (c) Bulatov, V.; Oref, I. *Int. J. Chem. Kinet.* **1993**, *25*, 1019–1028.

(9) (a) Frisch, M. J.; Trucks, G. W.; Schlegel, H. B.; Scuseria, G. E.; Robb, M. A.; Cheeseman, J. R.; Montgomery, J. A.; Vreven, T.; Kudin, K. N.; Burant, J. C.; Millam, J. M.; Iyengar, S. S.; Tomasi, J.; Barone, V.; Mennucci, B.; Cossi, M.; Scalmani, G.; Rega, N.; Petersson, G. A.; Nakatsuji, H.; Hada, M.; Ehara, M.; Toyota, K.; Fukuda, R.; Hasegawa, J.; Ishida, M.; Nakajima, T.; Honda, Y.; Kitao, O.; Nakai, H.; Klene, M.; Li, X.; Knox, J. E.; Hratchian, H. P.; Cross, J. B.; Bakken, V.; Adamo, C.; Jaramillo, J.; Gomperts, R.; Stratmann, R. E.; Yazyev, O.; Austin, A. J.; Cammi, R.; Pomelli, C.; Ochterski, J. W.; Ayala, P. Y.; Morokuma, K.; Voth, G. A.; Salvador, P.; Dannenberg, J. J.; Zakrzewski, V. G.; Dapprich, S.; Daniels, A. D.; Strain, M. C.; Farkas, O.; Malick, D. K.; Rabuck, A. D.; Raghavachari, K.; Foresman, J. B.; Ortiz, J. V.; Cui, Q.; Baboul, A. G.; Clifford, S.; Cioslowski, J.; Stefanov, B. B.; Liu, G.; Liashenko, A.; Piskorz, P.; Komaromi, I.; Martin, R. L.; Fox, D. J.; Keith, T.; Al-Laham, M. A.; Peng, C. Y.; Nanayakkara, A.; Challacombe, M.; Gill, P. M. W.; Johnson, B.; Chen, W.; Wong, M. W.; Gonzalez, C.; Pople, J. A. *Gaussian03, Revision C.02*; Gaussian, Inc.: Wallingford, CT, 2004. (b) Montgomery, J. A.; Frisch, M. J.; Ochterski, J. W.; Petersson, G. A. *J. Chem. Phys.* **1999**, *110*, 2822–2827.

(10) Yamaguchi, K.; Takahara, Y.; Fueno, T.; Houk, K. N. *Theor Chim Acta* **1988**, *73*, 337–364.

for a set of electrocyclic ring openings, sigmatropic shifts, cycloreversions, and cycloaddition reactions.[13] Also, CBS-QB3 has a maximum error of 2.8 kcal/mol and average and mean absolute errors of 0.20 and 0.98 kcal/mol, respectively, for the G2 test set.[14] The CBS-QB3 energies presented should be taken as the most accurate.[15]

SCHEME 1. Cycloaddition and Ene Reaction Products for the Dimerization of 1[a]

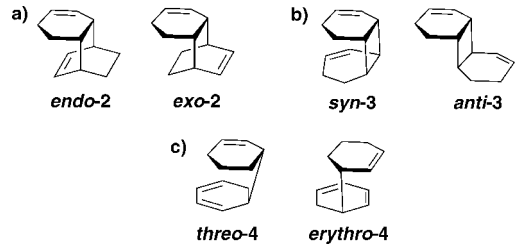

[a] (a) [4 + 2] cycloadducts, (b) [2 + 2] cycloadducts, and (c) [6 + 4] ene reaction products.

SCHEME 2. Possible Interactions for Cyclohexadiene and Cyclopentadiene Dimerization[a]

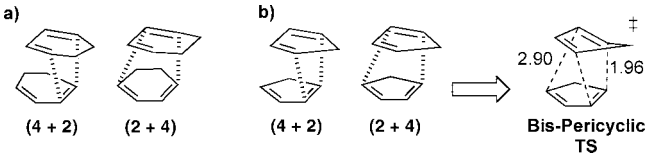

[a] Possible (4 + 2) and (2 + 4) interactions for (a) cyclohexadiene and (b) cyclopentadiene dimerization and the resulting B3LYP/6-31G(d) bis-pericyclic Diels−Alder transition state located by Caramella and coworkers.[4a]

SCHEME 3. Stepwise Reaction Pathways

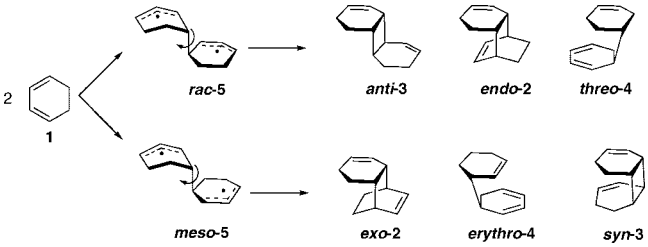

Results and Discussion

The groups of Klärner and Doering have studied the pressure and temperature dependency of 1,3-cyclohexadiene dimerization.[8,16] At temperatures above 150 °C, dimerization of **1** leads exclusively to a mixture of *endo*- and *exo*-[4 + 2] cycloadducts, ***endo*-2** and ***exo*-2** (Scheme 1a, Table 1). The CBS-QB3 ΔH_{0K} reaction enthalpies for the formation of ***endo*-2** and ***exo*-2** are −30.4 and −29.7 kcal/mol, respectively (Table 2). B3LYP predicts much less exothermic reaction enthalpies of −16.9 and −16.6 kcal/mol. Below 150 °C, a mixture of ***endo*-2**, ***exo*-2**, and the *syn*- and *anti*-[2 + 2] cycloadducts (***syn*-3** and ***anti*-3**), as well as an unprecedented [6 + 4] ene reaction product (***threo*-4**) were found in a ratio of 74:11:4:3:8 (Table 1 and Scheme 1b,c). The alternative [6 + 4] ene reaction product ***erythro*-4** was not observed (Scheme 1c). The B3LYP ΔH_{0K} enthalpies for ***syn*-3** and ***anti*-3** are −5.2 and −9.4 kcal/mol (Table 3). The CBS-QB3 $\Delta H_{(0K)}$ for ***syn*-3** and ***anti*-3** are −13.9 and −17.5 kcal/mol and the $\Delta G_{(298K)}$ values are −0.2 and −4.0 kcal/mol. These reaction enthalpies indicate that at temperatures above 150 °C, it is likely that ***syn*-3** and ***anti*-3** isomerize to give the more thermodynamically stable [4 + 2] cycloadducts and ***threo*-4** disproportionates via a retro-ene reaction ($\Delta H_{0K(B3LYP)}$ = −11.6 kcal/mol).[8]

TABLE 1. Experimental Product Ratios, Activation Energies (E_a, kcal/mol), and Activation Volumes ($\Delta V^{\ddagger}$, cm³/mol) for the Dimerization of 1,3-Cyclohexadiene[8]

species	ratio	E_a	$\Delta V^{\ddagger}$
***endo*-2**	74	22.6	−28
***exo*-2**	11	24.2	−22
***threo*-4**	8	21.5	−32
***syn*-3**	4	24.3	−22
***anti*-3**	3	25.3	−18

TABLE 2. B3LYP/6-31G(d), CASPT2(8,8)/6-31G(d), and CBS-QB3 Activation and Reaction Energies for Concerted [4 + 2] Cycloaddition (kcal/mol)

	B3LYP			CBS-QB3		CASPT2
	ΔE	ΔH_{0K}	ΔG_{298K}	ΔH_{0K}	ΔG_{298K}	ΔE
***endo*-2TS**	27.2	28.7	41.7	19.0	32.0	17.9
***endo*-2**[a]	−21.9	−16.9	−2.7	−30.4	−16.2	
2-Cope TS	22.1	25.0	39.6	10.4	24.8	5.1
***exo*-2TS**	28.4	30.1	43.6	21.1	34.5	19.5
***exo*-2**	−21.5	−16.6	−2.4	−29.7	−15.6	

[a] There is also an alternative ring-flipped conformation 1.1 kcal/mol lower in energy.

TABLE 3. B3LYP/6-31G(d), CASPT2(8,8)/6-31G(d) Activation and Reaction Energies for [2 + 2] Cycloadditions (kcal/mol)

	UB3LYP			CASPT2
	ΔE	ΔH_{0K}	ΔG_{298K}	ΔE
***rac*-5TS**	30.2 (25.5)[a,b]	30.1 (25.4)[a,b]	42.3	22.3
***rac*-5**	17.6 (17.7)[a,c]	18.5 (18.6)[a,c]	30.4	10.3
***meso*-5TS**	26.2 (21.8)[a,d]	26.4 (22.0)[a,d]	38.7	17.5
***meso*-5**	16.8 (16.0)[a,e]	17.8 (17.0)[a,e]	30.3	8.9
***anti*-3TSstep**	19.4 (14.3)[a,f]	20.4 (15.3)[a,f]	33.8	
***anti*-3**	−13.3	−9.4	4.1	
***endo*-2TSstep**	22.2 (17.6)[a,g]	23.5 (19.1)[a,g]	37.2	
***exo*-2TSstep**	24.7(19.7)[a,h]	26.2 (21.2)[a,h]	40.0	
***syn*-3**	−9.4	−5.2	8.6	

[a] Spin-projected values. [b] $S^2 = 0.65$. [c] $S^2 = 1.05$. [d] $S^2 = 0.52$. [e] $S^2 = 1.03$. [f] $S^2 = 0.64$. [g] $S^2 = 0.66$. [h] $S^2 = 0.65$.

(11) (a) Andersson, K.; Malmqvist, P.; Roos, B. O. *J. Chem. Phys.* **1992**, *96*, 1281–1226. (b) Andersson, K.; Roos, B. O. In *Modern Electronic Structure Theory*; Yarkony, D. R., Ed.; World Scientific: Singapore, 1995; p 55. Implemented in Molcas, version 6.2.

(12) (a) Montgomery, J. A.; Frisch, M. J.; Ochterski, J. W.; Petersson, G. A. *J. Chem. Phys.* **2000**, *112*, 6532–6542. (b) Petersson, G. A.; Malick, D. K.; Wilson, W. G.; Ochterski, J. W.; Montgomery, J. A.; Frisch, M. J. *J. Chem. Phys.* **1998**, *109*, 10570–10579.

(13) (a) Guner, V.; Khuong, K. S.; Leach, A. G.; Lee, P. S.; Bartberger, M. D.; Houk, K. N. *J. Phys. Chem. A* **2003**, *107*, 11445–11459. (b) Ess, D. H.; Houk, K. N. *J. Phys. Chem. A* **2005**, *109*, 9542–9553.

(14) Curtiss, L. A.; Raghavachari, K.; Trucks, G. W.; Pople, J. A. *J. Chem. Phys.* **1991**, *94*, 7221–7230.

(15) (a) Grimme, S. *Angew. Chem., Int. Ed.* **2006**, *45*, 4460–4464. (b) Wodrich, M. D.; Corminboeuf, C.; Schleyer, P. v. R. *Org. Lett.* **2006**, *8*, 3631–3634. (c) Schreiner, P. R.; Fokin, A. A.; Pascal, R. A.; de Meijere, A. *Org. Lett.* **2006**, *8*, 3635–3638. (d) Check, C. E.; Gilbert, T. M. *J. Org. Chem.* **2005**, *70*, 9828–9834.

(16) (a) Schutte, R.; Freeman, G. R. *J. Am. Chem. Soc.* **1969**, *91*, 3715–3720. (b) Nakata, T.; Choumei, N. J. *J. Macromol. Sci., Pure Appl. Chem.* **1967**, *A1* (8), 1433–1442. (c) Stroebel, G. G.; Myers, D. Y.; Grabbe, R. R.; Gardner, P. D. *J. Phys. Chem.* **1978**, *82*, 1121–1125. (d) Asaoka, S.; Ooi, M.; Jian, P.; Wada, T.; Inoue, Y. *J. Chem. Soc., Perkin Trans. 2* **2000**, 77–84. (e) Amerik, A. B.; Vdovin, V. H. *Ser. Khim.* **1979**, *4*, 907–910. (f) Takeshita, H.; Sugiyama, S.; Hatsui, T. *J. Chem. Soc., Perkin Trans. 2* **1986**, 1491–1494. (g) Calhoun, G. C.; Schuster, G. B. *Tetrahedron Lett.* **1986**, *27*, 911–914. (h) Lin, C.-H.; Lee, C.-Y.; Liu, C.-S. *J. Am. Chem. Soc.* **1986**, *108*, 1323–1325. (i) Calhoun, G. C.; Schuster, G. B. *J. Am. Chem. Soc.* **1984**, *106*, 6870–6871. (j) Valentine, D.; Turro, N. J.; Hammond, G. S. *J. Am. Chem. Soc.* **1964**, *86*, 5202–5208.

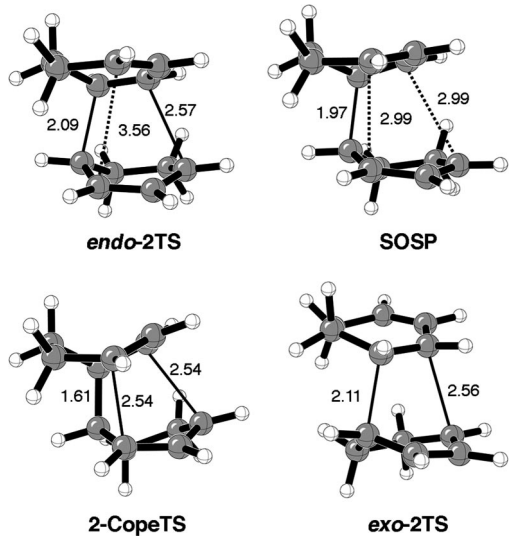

FIGURE 1. Concerted *endo*-[4 + 2], second-order, Cope, and *exo*-[4 + 2] transition states for cyclohexadiene dimerization.

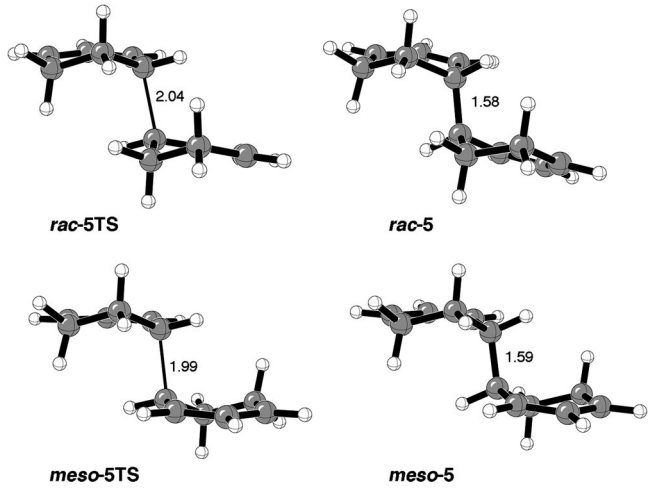

FIGURE 2. Diradical transition states leading to ***rac*-5** and ***meso*-5** intermediates.

Table 1 also gives the experimentally measured activation energies (E_a) over the temperature range of 70−150 °C, and the activation volumes ($\Delta V^{\ddagger}$), the difference in partial molar volume of the transition state and the reactants, measured over a pressure range of 1−7000 bar at 70 °C.

[4 + 2] Cycloaddition Transition States. Figure 1 shows the concerted B3LYP [4 + 2] cycloaddition transition, ***endo*-2TS**.[17] This transition state is moderately asynchronous with forming partial bond lengths of 2.09 Å and 2.57 Å. Surprisingly, ***endo*-2TS** lacks the expected C_s symmetry that is found for cyclopentadiene, butadiene, and several other *endo* diene cycloaddition transition states. Scheme 2 shows that a superficial analysis of possible orbital interactions of cyclohexadiene dimerization (Scheme 2a) would involve the same interactions that occur in cyclopentadiene dimerization (Scheme 2b). C_s symmetry in the cyclopentadiene transition state simultaneously maximizes primary and secondary interactions (which are equally involved in a bis-pericyclic transition state). Contrary to expectation, two equivalent

(17) The alternative ring-flipped Diels−Alder transition state is 0.9 kcal/mol higher in energy.

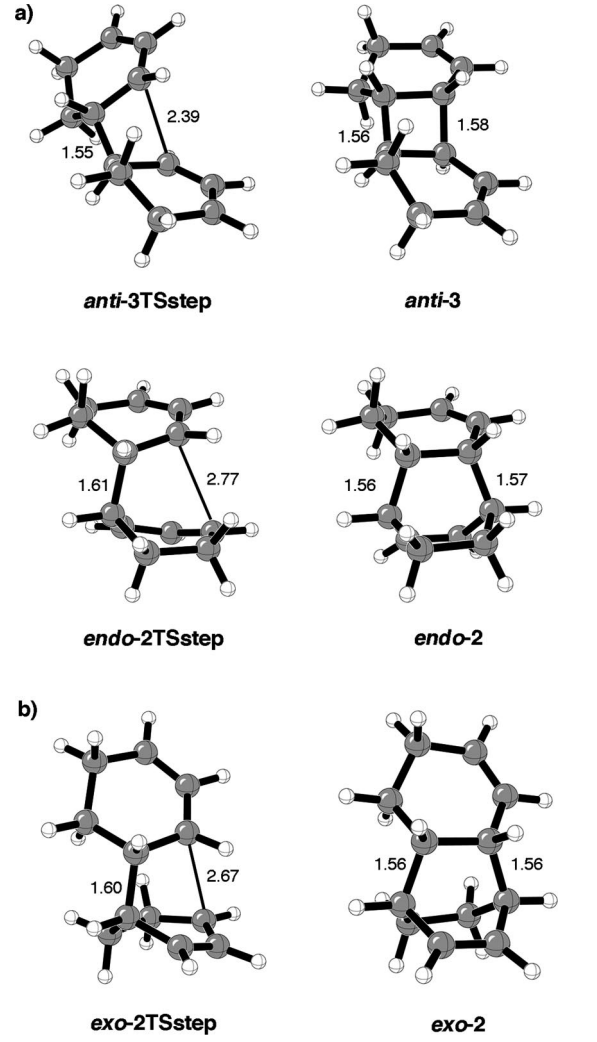

FIGURE 3. Ring-closing diradical transition states and cycloadducts resulting from (a) ***rac*-5** and (b) ***meso*-5**.

Diels−Alder [4 + 2] and [2 + 4] transition states exist for *endo* cyclohexadiene dimerization, rather than a single bis-pericyclic transition state.[18,19] Therefore, one cyclohexadiene formally acts as the diene fragment while the other acts as the dienophile.

The ***endo*-2TS** transition state breaks symmetry due to intramolecular methylene group eclipsing interactions and intermolecular methylene group repulsions. However, the expected C_s symmetry structure is a second-order saddle point (**SOSP**, Figure 1) that is only 0.3 kcal/mol higher in energy than ***endo*-2TS** and connects equivalent forms of ***endo*-2TS**.[20] The **SOSP** begins a ridge region that divides the [4 + 2] and the [2 + 4] addition reaction pathways until they merge at the Cope transition state, **2-CopeTS**, which also has C_s symmetry with degenerate partial bond lengths of 2.54 Å (Figure 1). The significant change in geometry between ***endo*-**

(18) (a) Carpenter, B. K. In *Reactive Intermediate Chemistry*; Moss, R. A., Platz, M. S., Jones, M., Eds.; Wiley-Interscience: Hoboken, NJ, 2004; pp 925−960. (b) Kraka, E. In *Encyclopedia of Computational Chemistry*; Schleyer, P. v. R., Ed.; Wiley: New York, 1998; Vol. 4, p 2445. (c) Valtazanos, P.; Elbert, S. T.; Ruedenberg, K. *J. Am. Chem. Soc.* **1986**, *108*, 3147–3149. (d) Valtazanos, P.; Ruedenberg, K. *Theor. Chim. Acta* **1986**, *69*, 281–307. (e) Quapp, W.; Hirsch, M.; Heidrich, D. *Theor. Chem. Acc.* **1998**, *100*, 285–299.

(19) Singleton, D. A.; Hang, C.; Szymanski, M. J.; Meyer, M. P.; Leach, A. G.; Kuwata, K. T.; Chen, J. S.; Greer, A.; Foote, C. S.; Houk, K. N. *J. Am. Chem. Soc.* **2003**, *125*, 1319–1328.

SCHEME 4. Comparison of Concerted and Stepwise Potential Energy Surfaces ($\Delta H_{0K(B3LYP)}$, kcal/mol)

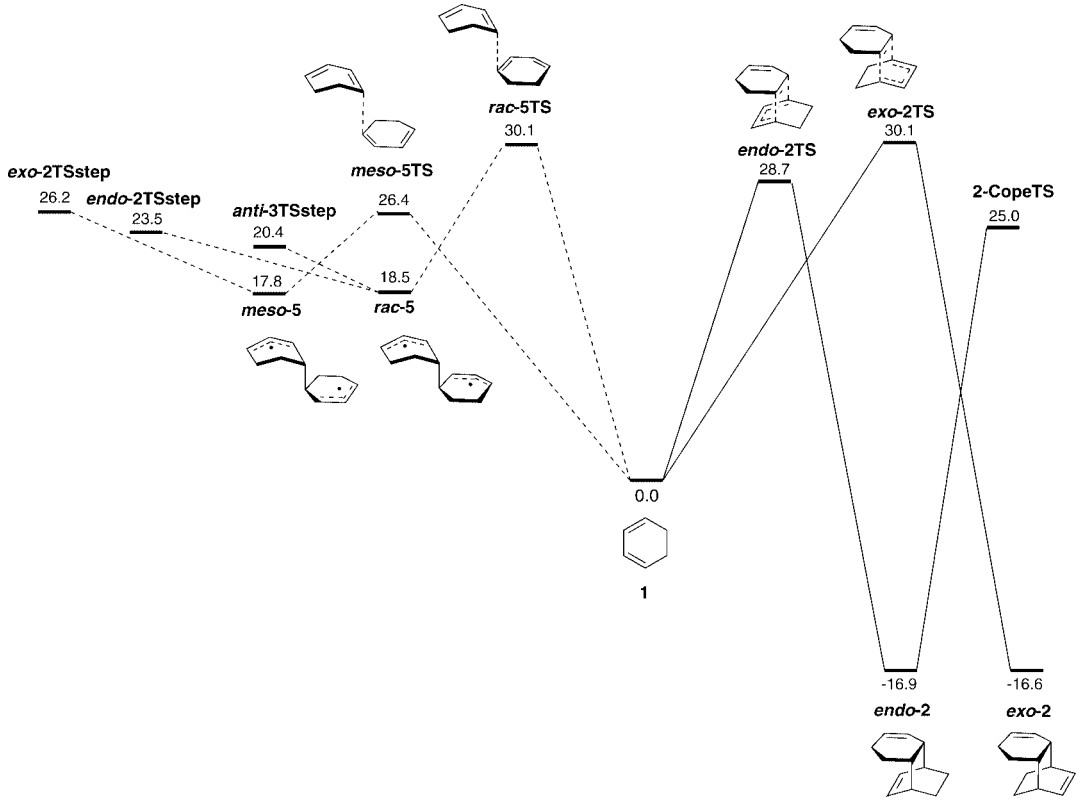

SCHEME 5. More O'Ferrall−Jencks Structure Comparison to the Concerted B3LYP Ene Transition State for *cis*-Butadiene with *cis*-Methylbutadiene

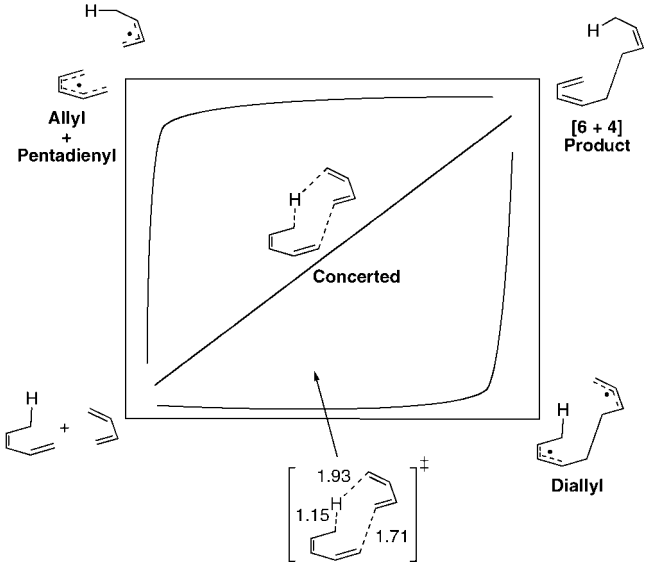

SCHEME 6. Possible Sigmatropic [3,3] Sigmatropic Rearrangements

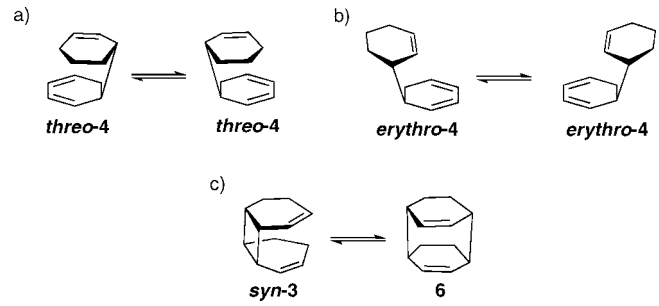

2TS and **SOSP** with a small energy change indicates a very flat energy surface. In fact, the barrier between these first- and second-order saddle points is so low that this reaction is best described as quasi bis-pericyclic, because zero-point energy effects may be larger than the **SOSP** energy.[21,22] The transition state region effectively acts like a bis-pericyclic transition state. We speculate that a similar type of potential energy surface may exist for several other endo dimerizations.[6]

The lack of strong secondary orbital interactions combined with larger geometric distortion required in ***endo*-2TS** results in a ~10 kcal/mol larger activation barrier when compared with other cyclic and acyclic *endo* dimerizations. B3LYP overestimates the activation barrier ($\Delta H^{\ddagger}_{0K}$ = 28.7 kcal/mol, Table 2) by ~6 kcal/mol when compared with the experimental values reported by Klärner et al. and Huybrechts et al., 22.6 ± 0.5 and 23.2 kcal/mol, respectively.[8,23] CBS-QB3

(20) (a) The UB3LYP energy solution to **SOSP** is 0.1 kcal/mol below the RB3LYP solution and $S^2 = 0.005$. (b) The negative eigenvalues for **SOSP** are −421 and −71 cm^{-1}. (c) Larger 6-31+G(d,p) and 6-311G(d,p) basis sets also give unsymmetrical Diels−Alder transition states. (d) Hartree-Fock and density functional methods (pure and hybrid) converged on non bis-pericyclic transition state geometries. Hartree-Fock/6-31G(d) gave the most asynchronous structure with partial bond lengths of 2.149, 2.312, and 3.716 Å, whereas the bp86/6-31G(d) method gave a nearly symmetrical structure with bond lengths of 2.064, 3.028, and 3.034 Å. Only the MP2/6-31G(d) method gave a C_s symmetric Diels−Alder structure with bond lengths of 2.131, 2.850, and 2.850 Å. The MP2 Cope structure has bond lengths of 1.583, 2.278, and 2.279 Å (see Supporting Information and ref 22).

(21) On the electronic BLYP/6-31G(d) energy surface, the second-order saddle point (bond lengths = 1.96, 3.11, 3.11 Å) is only 0.1 kcal/mol above the Diels-Alder transition state (bond lengths = 2.01, 2.82, 3.46 Å). With zero-point corrections, the second-order saddle is then 0.1 kcal/mol below the Diels−Alder transition state.

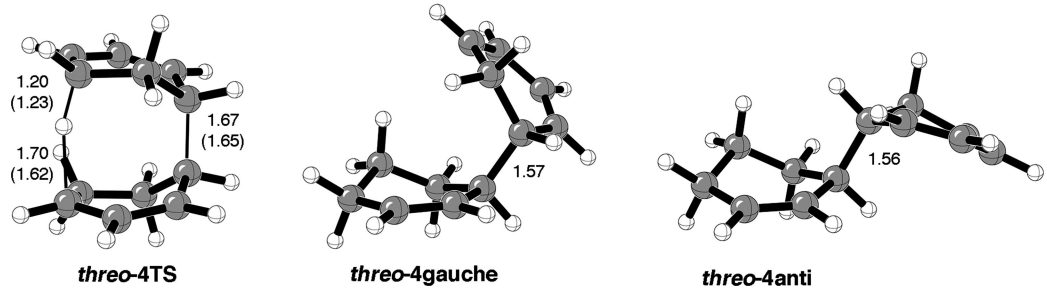

FIGURE 4. [6 + 4] Ene reaction transition state and products.

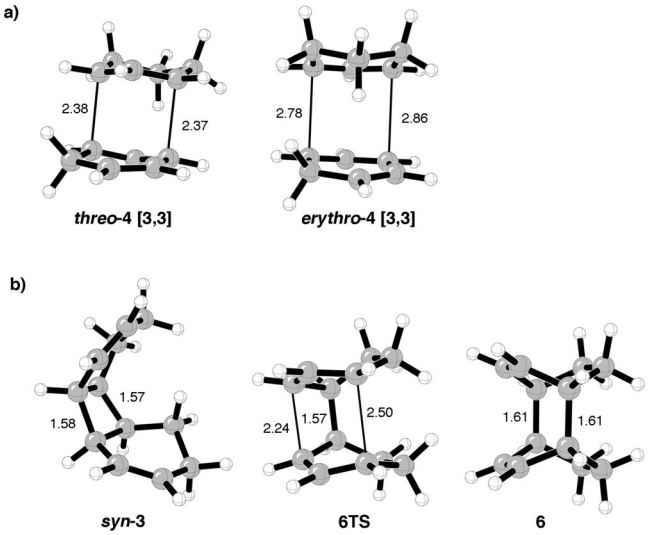

FIGURE 5. (a) [3,3] Sigmatropic rearrangement transition structures for ***threo*-4** and ***erythro*-4**. (b) Minima and transition structure for rearrangement of ***syn*-3** to **6**.

and CASPT2(8,8)/6-31G(d) give reasonable agreement with experiment and predict barriers of 19.0 and 17.9 kcal/mol (Table 2). B3LYP, CBS-QB3, and CASPT2 all predict ***endo*-2TS** to be the lowest energy transition state for all concerted processes.

The exo concerted [4 + 2] cycloaddition transition structure, ***exo*-2TS**, is nearly as synchronous as ***endo*-2TS** with partial bond lengths of 2.36 and 2.56 Å, but it is 1.4 kcal/mol higher in energy ($\Delta H^{\ddagger}_{0K}$ = 30.1 kcal/mol) due to repulsive methylene-methylene group interactions and no stabilizing secondary orbital interactions. Although CBS-QB3 and CASPT2 both predict a similar energy difference between ***exo*-2TS** and ***endo*-2TS**, the predicted barrier heights are substantially lower than the B3LYP value (see Table 2).

[2 + 2] Cycloaddition Transition States. As a result of orbital symmetry constraints, the [2 + 2] cycloadducts, ***syn*-3** and ***anti*-3**, are formed via diradical transition states.[24] Domingo and co-workers have previously studied part of the photochemical triplet reaction surface.[25] Scheme 3 shows the two possible diallyl diradical intermediates, as well as the cycloaddition and ene products, that are possible from each intermediate after C−C bond rotation followed by ring closure or hydrogen abstraction.

Figure 2 shows the stepwise transition states ***rac*-5TS** and ***meso*-5TS** along with their corresponding intermediates, ***rac*-5** and ***meso*-5**. The B3LYP $\Delta H^{\ddagger}_{0K}$ for ***meso*-5TS** is 26.4 kcal/mol, and spin-projection lowers the barrier to 22.0 kcal/mol (Table 3), which is close to the barrier of 24.3 kcal/mol measured for ***syn*-3**. The activation enthalpy for ***rac*-5TS** is 3.7 kcal/mol higher in energy (25.4 kcal/mol with spin-projection) due to gauche methylene-methylene group interactions between cyclohexadiene ring fragments, while ***meso*-5TS** has an ideal *anti* conformation about the newly forming C−C bond. CASPT2 gives barriers of 17.5 and 22.3 kcal/mol for ***meso*-5TS** and ***rac*-5TS**, respectively. The barrier measured for ***anti*-3** is 25.3 kcal/mol, only 1.0 kcal/mol higher than the barrier for ***syn*-3**. B3LYP and CASPT2 agree that there is a substantial barrier difference ***meso*-5TS** and ***rac*-5TS**. The discrepancy between theory and experiment remains unclear. However, it should be noted that the activation volumes for ***syn*-3** and ***exo*-2** are measured to be 4 cm^3/mol more negative than for ***anti*-3**, which arises from ***rac*-5TS**, even though qualitatively ***meso*-5TS** should have a less negative activation volume. The ***rac*-5** and ***meso*-5** intermediates are nearly equi-energetic ($\Delta H_{0K} \approx 18$ kcal/mol).

Rotation about the newly formed C−C bond in ***rac*-5** by ∼35° leads to ***anti*-3** though transition state ***anti*-3TSstep** with a barrier of 1.9 kcal/mol (Figure 3a). Further rotation of ***rac*-5** allows ***endo*-2** to be formed via ***endo*-2TSstep** with an enthalpic barrier of 5.0 kcal/mol (Figure 3a). This alternative stepwise pathway (compared to the concerted pathway) is likely controlled by the dynamic influences of bypassing ***anti*-3** formation. Rotation by a total of ∼215° in ***rac*-5** (or 100° in the opposite direction) would result in a geometry similar to that of ***threo*-4TS**. However, rotation this far may be unlikely.

The barrier to form the intermediate ***meso*-5** is computed to be the lowest of all transition states and likely gives rise to much of the polymerization product observed experimentally after disproportionation.[8] Scheme 3 shows that ***meso*-5** can hypothetically lead to ***exo*-2**, ***syn*-3**, and ***erythro*-4**. However, no transition state for the hydrogen abstraction leading to ***erythro*-4** was found (nor was a concerted transition state found) as a result of severe methylene-methylene group repulsive interactions between the two cyclohexadiene fragments.[26] All attempts to find a transition structure leading to ***syn*-3** resulted in a transition state for dyotropic hydrogen group transfer between cyclohexadienes. A possible alternate route for formation of ***syn*-3** is via stepwise formation of the [4 + 4] cycloadduct **6** followed by a [3,3] sigmatropic shift (see later discussion). Rotation of the newly formed C−C

(22) Yaghmaei, S.; Khodagholian, S.; Kaiser, J. M.; Mueller, L. J.; Morton, T. H. *J. Am. Chem. Soc.* **2008**, *130*, 7836–7838.

(23) The reported values are activation energies, $E_a = H + nRT$. We have not corrected for this minor change.

(24) Intermolecular hydrogen abstraction is unlikely because the bond dissociation enthalpy is 78.6 kcal/mol. Also see: (a) Agapito, F.; Nunes, P. M.; Cabral, B. J. C.; Borges dos Santos, R. M.; Simões, J. A. M. *J. Org. Chem.* **2007**, *72*, 8770–8779. (b) Nunes, P. M.; Agapito, F.; Cabral, B. J. C.; Borges dos Santos, R. M.; Simões, J. A. M. *J. Phys. Chem A* **2006**, *110*, 5130–5134.

(25) Domingo, L. R.; Pérez-Prieto, J. *Chem. Phys. Chem.* **2006**, *7*, 614–618.

bond in ***meso*-5** by ~136° leads to ***exo*-2TSstep** that has an enthalpic barrier of 8.4 kcal/mol (Figure 3b).

Scheme 4 shows a composite potential energy surface comparing concerted and stepwise processes. The activation volumes measured for ***endo*-2** ($\Delta V^{\ddagger} = -28$ cm^3/mol) and ***exo*-2** ($\Delta V^{\ddagger} = -22$ cm^3/mol) suggest that the *endo*-[4 + 2] cycloadduct is formed via a highly ordered, concerted transition state, while the *exo*-[4 + 2] cycloadduct is formed via a much less ordered, diradical transition state. This is consistent with the concerted ***exo*-2TS** being higher in energy than the alternative stepwise pathway that proceeds through ***meso*-5TS** and subsequently though ***exo*-2TSstep**. Cycloadduct ***endo*-2** is formed only via the concerted transition state ***endo*-2TS**.

[6 + 4] Ene Reaction. The [6 + 4] ene reaction product, ***threo*-4**, observed by Klärner, is an unprecedented 10-electron ene reaction involving two 4-electron π-systems and a C−H σ-bond. Ene reaction transition state geometries generally differ greatly depending on reactants and substitution.[27] Scheme 5 shows the More O'Ferrall−Jencks structures for the model acyclic system reaction of *cis*-butadiene with *cis*-methylbutadiene as the enophile. In the RB3LYP transition structure, the forming C−C bond is nearly complete with a bond length of 1.71Å, while the breaking C−H bond is lengthened to 1.15Å. The ene transition state for cyclohexadiene, ***threo*-4TS** (Figure 4), has a slightly shorter C−C bond distance (1.67 Å) and a longer breaking C−H bond (1.20 Å).[28] Both of these transition states closely resemble the diallyl diradical species in Scheme 5a. Although the model transition state has a stable closed-shell RB3LYP solution, ***threo*-4TS** is more stable when computed with unrestricted theory. Reoptimization with UB3LYP gives an even shorter C−C (1.65 Å) and forming C−H (1.62 Å) bond lengths and an even longer C−H cleavage bond length (1.23 Å, see Figure 4). The UB3LYP activation enthalpy at 0 K is 28.3 kcal/mol, 0.3 kcal/mol below the RB3LYP solution, with a S^2 value is 0.17, indicating a slight mixture of singlet and triplet states. Spin-projection lowers the activation enthalpy to 26.5 kcal/mol. The compact *endo* nature of ***threo*-4TS** fits with the observed activation volume measurement of −32 cm^3/mol and is the primary reaction pathway for ***threo*-4** formation, rather than via the ***rac*-5** intermediate followed by C−C bond rotation and hydrogen abstraction. Transition state ***threo*-4TS** leads to the gauche conformation of ***threo*-4** and there a 7 kcal/mol barrier is required for rotation to the more stable *anti* conformation (Figure 4).

Similar diradicaloid transition states have also been identified in other 10-electron pericyclic reactions[29] and in the ene reaction of cyclopropene dimerization.[30] Houk and coworkers have shown that the propensity toward diradical ene transition structures is related to the heats of formation for the diradical species and the degree of strain required for a concerted transition state.[13]

[3,3] Sigmatropic Rearrangement Transition States. Several [3,3] sigmatropic shift transition states were located that have activation barriers similar in magnitude to cycloaddition and ene reaction barriers. Scheme 6 shows three rearrangement pathways. The first two (Scheme 6a,b) interconvert equivalent forms of ***threo*-4** and ***erythro*-4**, while the third (Scheme 6c) converts ***syn*-3** into the formal [4 + 4] cycloadduct, **6**. The transition structures for each of these processes are shown in Figure 5. The rearrangement of ***threo*-4** has an activation enthalpy of 27.1 kcal/mol, making this process likely to occur under reaction conditions. The barrier for ***erythro*-4** rearrangement is 31.1 kcal/mol and has significantly longer partial bond lengths in the transition state. Although not observed experimentally, there is a relatively low barrier (29.3 kcal/mol) for conversion of ***syn*-3** to **6** via transition state **6TS**. However, it is possible that **6** was not observed experimentally because ***syn*-3** is significantly more thermodynamically stable ($\Delta\Delta H_{\mathrm{B3LYP(0K)}} = -7.7$ kcal/mol).

Conclusion

B3LYP, CASPT2, and CBS-QB3 methods have been used to explore concerted and stepwise processes involved in cyclohexadiene dimerization. The *endo*-[4 + 2] cycloadduct is formed through a concerted, non-bis-pericyclic transition state, while the *exo*-[4 + 2] cycloadduct is formed through a diradical stepwise pathway. The novel [6 + 4] ene reaction product is the result of a highly asynchronous, although concerted, diradicaloid transition state.

Acknowledgment. We are grateful to the National Science Foundation for financial and supercomputer support. The computations were performed using National Center for Supercomputing Applications (NCSA) resources and the UCLA Academic Technology Services (ATS) Hoffman Beowulf cluster. Thanks to Lai Xu for help with supercomputer time.

Supporting Information Available: Absolute energies and Cartesian coordinates of stationary points. This material is free of charge via the Internet at http://pubs.acs.org.

JO8011804

(26) The barrier for hydrogen abstraction at the alternative γ-carbon has a $\Delta H^{\ddagger}_{0K} = 45.2$ kcal/mol. ***threo*-4** hydrogen abstraction at the γ radical also requires a much larger activation enthalpy, and abstraction at the β-carbon does not occur because this would result in the formation of a high energy triradical.

(27) (a) Loncharich, R. J.; Houk, K. N. *J. Am. Chem. Soc.* **1987**, *109*, 6947–6952. (b) Deng, Q.; Thomas, B. E.; Houk, K. N.; Dowd, P. *J. Am. Chem. Soc.* **1997**, *119*, 6902–6908. (c) Typical B3LYP transition structure bond lengths: forming the C-C bond, 2.11 Å; forming the C−H bond, 1.48 Å; and breaking the C−H bond, 1.32 Å.

(28) Yamabe, S.; Tsuchida, N.; Yamazaki, S. *J. Chem. Theory Comput.* **2005**, *1*, 944–952.

(29) Chen, Y.; Ye, S.; Jiao, L.; Liang, Y.; Sinha-Mahapatra, S.; Hendron, J. W.; Yu, Z.-X. *J. Am. Chem. Soc.* **2007**, *129*, 10773–10784.

(30) (a) Beno, B. R.; Fennen, J.; Houk, K. N.; Lindner, H. J.; Hafner, K. *J. Am. Chem. Soc.* **1998**, *120*, 10490–10493. (b) Leach, A. G.; Houk, K. N. *J. Am. Chem. Soc.* **2002**, *124*, 14820–14821.